








Original Research

# Irisolidone Ameliorates Cyclophosphamide-Induced POI via Inhibiting Inflammatory Response

Mingjin Li<sup>1</sup>, Zhenhong Wei<sup>2</sup>, Xiaohong Chen<sup>1</sup>, Huifang Wu<sup>1</sup>, Xue Han<sup>1</sup>,  
Yaping Pei<sup>1</sup>, Jiyu Chen<sup>3,4</sup>, Shouye Ma<sup>1,\*</sup>

<sup>1</sup>Department of Gynecology and Obstetrics, Gansu Provincial Hospital & The Third Hospital of Lanzhou University, 730000 Lanzhou, Gansu, China

<sup>2</sup>The Institute of Clinical Research and Translational Medicine, Gansu Provincial Hospital & The Third Hospital of Lanzhou University, 730000 Lanzhou, Gansu, China

<sup>3</sup>Clinical Trials Center, The Affiliated Hospital of Guizhou Medical University, 550000 Guiyang, Guizhou, China

<sup>4</sup>Department of Pharmacy, Clinical Research Center of Integrated Traditional Chinese and Western Medicine, 550000 Guiyang, Guizhou, China

\*Correspondence: [msymashouye@163.com](mailto:msymashouye@163.com) (Shouye Ma)

Academic Editor: Graham Pawelec

Submitted: 12 August 2025 Revised: 8 October 2025 Accepted: 7 November 2025 Published: 26 November 2025

## Abstract

**Background:** Premature ovarian insufficiency (POI) is a condition marked by diminished ovarian function and reduced fertility, caused by the chemotherapy drug cyclophosphamide (CTX) used to treat gynecologic cancers. The abnormal inflammation of ovarian tissue induced by CTX represents a key factor that impairs follicular cells and disrupts fertility. Therefore, the present study aims to investigate the underlying mechanisms of CTX-induced abnormal ovarian inflammation and identify potential therapeutic agents. **Methods:** RNA sequencing data derived from CTX-induced mouse ovarian tissues were first intersected with inflammation-related genes retrieved from the Gene Ontology (GO) database. This was followed by functional enrichments analysis and protein-protein interaction (PPI) analyses to identify target genes. Subsequently, the Traditional Chinese Medicine Systems Pharmacology Database and Analysis Platform (TCMSP) was screened to obtain corresponding candidate therapeutic agents. Finally, a CTX-induced mouse model was established to verify the therapeutic efficacy of the candidate drug and elucidates its underlying mechanisms. **Results:** A total of 25 candidate genes were identified, with interleukin 1 $\beta$  (IL1 $\beta$ ) confirmed as the core gene. Subsequent screening resulted in the identification of Irisolidone as a potential therapeutic agent. The present study demonstrated that Irisolidone ameliorates CTX-induced follicular cell developmental impairment and improves fertility in mice with POI. Mechanistically, it was found that Irisolidone suppressed abnormal ovarian inflammation by inhibiting the CTX-disrupted nuclear factor kappa B (NF $\kappa$ B)/NOD-like receptor pyrin domain-containing 3 (NLRP3)/Caspase1 signaling pathway. **Conclusion:** The present study demonstrates that Irisolidone can effectively alleviate CTX-induced POI by inhibiting abnormal inflammation. These findings suggest that Irisolidone holds promise as a novel therapeutic candidate for POI, thereby providing a potential new treatment strategy for clinical management of this condition.

**Keywords:** premature ovarian insufficiency; cyclophosphamide; Irisolidone; inflammation; Chinese traditional medicine

## 1. Introduction

Premature ovarian insufficiency (POI) is a clinical syndrome defined by impaired ovarian function and reduced fertility, with an incidence of approximately 1–5% among women [1,2]. Clinical manifestations of POI include menstrual irregularities and infertility, and the condition is frequently associated with anxiety, memory impairment, and osteoporosis [3,4]. The etiology of POI is complex, encompassing factors such as inflammation, genetic variations, environmental exposures, and underlying medical conditions [5]. Therefore, exploring the potential mechanisms and therapeutic targets for POI is urgent.

Worldwide, roughly 9 million women receive a cancer diagnosis annually. Of these cases, breast cancer is the most prevalent, with colorectal cancer and cervical cancer ranking second and third, respectively [6]. Chemotherapy is a pivotal approach for the treatment and control of cancer; however, due to their poor targeting, chemotherapeutic

agents can damage normal tissues while eliminating cancer cells [7]. Clinically, cyclophosphamide (CTX)-widely used in the treatment of gynecological cancers-can induce damage to ovarian cells, leading to impaired ovarian function and infertility [8]. Additionally, embryo cryopreservation represents a viable option for young patients with POI, but this technique is associated with inherent risks and high costs [9]. Therefore, there is an urgent need to explore additional potential therapeutic agents.

The onset and progression of POI are associated with multiple factors, among which an inflammatory microenvironment within the ovaries serves as a key mediator of ovarian dysfunction. Dysregulation of inflammatory cytokines can affect follicular development and ovulation, ultimately leading to the development of POI and subsequently infertility [10,11]. CTX treatment is known to induce inflammatory abnormalities in multiple organs, including the heart, kidneys, and lungs [12–14]. Importantly,



the persistent inflammation triggered by CTX can drive cellular senescence and functional impairment of normal ovarian cells [15]. Therefore, the identification of novel anti-inflammatory agents may provide potential therapeutic options for the clinical management of POI.

Given the potential relationship between POI and abnormal inflammation, the present study aims to identify shared therapeutic targets by integrating the screening of POI-related risk factors and inflammatory risk factors. Subsequently, potential compounds with anti-inflammatory properties will be screened from a natural product library, followed by validation in a CTX-induced POI mouse model. In summary, this study seeks to identify novel candidate therapeutic agents, thereby providing new strategies for the clinical treatment of POI.

## 2. Materials and Methods

### 2.1 Animals

All animal experiments were conducted in accordance with the National Institutes of Health (NIH) Guide for the Care and Use of Laboratory Animals (NIH Publication No. 80-23; revised 1978). The protocol for all animal experiments was approved by the Animal Experimental Ethical Inspection Form at Guizhou Medical University (No. 12403436). Seven-week-old female C57BL/6 mice were obtained from GemPharmatech Co., Ltd. (Nanjing, Jiangsu, China) and allowed to acclimate to the new environment for one week, with free access to standard chow and water throughout the acclimation period. Female mice were housed in a specific pathogen-free (SPF) facility, maintained under a 12-hour light/dark cycle, humidity 10–70%, temperature of 20–25 °C, and free access to standard chow and water.

### 2.2 Mouse Model

The animals were randomly divided into four groups ( $n = 10$  per group): (1) Sham + Vehicle group, (2) Sham + Irisolidone group, (3) POI + Vehicle group, and (4) POI + Irisolidone group. Female mice in the POI group (Groups 3 and 4) received a single intraperitoneal injection of cyclophosphamide (CTX, 100 mg/kg, Selleck, Cat. NO. S1217, CAS No: 50-18-0) to induce a POI model. Female mice in the control group (Groups 1 and 2) received an equivalent volume of vehicle solution *via* intraperitoneal injection. Subsequently, female mice in the Irisolidone-treated groups (Groups 2 and 4) received daily intraperitoneal injections of Irisolidone (50 mg/kg, BioBioPha, BBP No: BBP06887, CAS No: 2345-17-7) for three consecutive weeks.

At the end of the treatment period, female mice were anesthetized with 3% pentobarbital sodium (60 mg/kg) *via* intraperitoneal injection, followed by cardiac blood collection. After transcardial perfusion with physiological saline, ovaries were harvested. Ovarian tissues and serum samples (separated from collected blood) were stored appropriately for subsequent experimental analyses.

### 2.3 Public Data Analysis

The ovarian RNA sequencing data for the CTX-induced POI mouse model were obtained from the Gene Expression Omnibus (GEO, <https://www.ncbi.nlm.nih.gov/gds/>) database under accession number GSE128240 [16]. The inflammation-related gene datasets were retrieved from the “Inflammatory Response” pathway within the Gene Ontology (GO) database. To identify candidate genes, GO enrichment analysis was performed using Metascape (<https://metascape.org/>), a comprehensive tool for functional annotation and gene lists analysis. For pathway analysis, the Database for Annotation, Visualization, and Integrated Discovery (DAVID, <https://davidbioinformatics.nih.gov/>) is utilized to conduct Kyoto Encyclopedia of Genes and Genomes (KEGG, <https://www.genome.jp/kegg/>) functional enrichment analysis. The candidate genes were subjected to Protein-Protein Interaction (PPI) analysis using Cytoscape software (National Resource for Network Biology, San Diego, CA, USA) to identify core proteins. Additionally, the conservation of interleukin 1 $\beta$  (IL1 $\beta$ ) protein motif sites across species was performed to use Gene Set Enrichment Analysis (GSEA, <https://www.gsea-msigdb.org/gsea/index.jsp>).

### 2.4 Natural Drug Screen

Natural compounds with anti-inflammatory properties were initially screened using the Traditional Chinese Medicine Systems Pharmacology (TCMSP, [https://www.tcm-sp-e.com/load\\_intro.php?id=43](https://www.tcm-sp-e.com/load_intro.php?id=43)) database [17,18]. Subsequently, the compound library was further refined based on drug-like properties, including absorption, distribution, metabolism, and excretion (ADME), molecular weight, oral bioavailability, drug half-life, and other pharmacokinetic parameters. This refinement process identified potential drug candidates with favorable pharmaceutical properties. Finally, Molecular Operating Environment (MOE, Chemical Computing Group, Montreal, Canada) software was utilized to perform molecular docking simulations of these druggable compounds, aiming to evaluate their binding affinity to the target protein IL1 $\beta$ . This comprehensive screening strategy enabled the identification of promising natural compounds.

### 2.5 Histological Analysis

Following collecting, ovarian tissues were immediately fixed in 4% paraformaldehyde at room temperature overnight. The fixed tissues were then processed for paraffin embedding, followed by sectioning into 5  $\mu$ m-thick slices. Hematoxylin and Eosin (H&E) staining was performed on these sections to assess histological structure. Subsequently, based on established ovarian cell classification criteria, follicles at different developmental stages—including primordial, primary, secondary, antral, and atretic follicles—were identified and quantified [19].

## 2.6 Immunostaining Assay

The Immunohistochemistry (IHC) staining procedure is as follows: Ovarian tissue sections were dewaxed and subjected to antigen retrieval. After cooling, the sections were incubated with 3% hydrogen peroxide for 10–15 minutes to block endogenous peroxidase activity, followed by blocking with 5% BSA for 30 minutes. phosphorylated nuclear factor kappa B (*p*-NF $\kappa$ B; 1:200, Proteintech, Cat. No. 10745-1-AP, Wuhan, Hubei, China), NOD-like receptor pyrin domain-containing 3 (NLRP3; 1:200, ABclonal, Cat. No. A5652, Wuhan, Hubei, China), and Caspase1 (1:200, Proteintech, Cat No. 22915-1-AP, Wuhan, China) were added, and the sections were incubated overnight at 4 °C. Subsequent to this, the sections were incubated with the polymer HRP-goat anti-rabbit recombinant secondary antibody (H+L) (Cat: RGAR011, Proteintech, Wuhan, China) at room temperature for 60 minutes. 3,3'-Diaminobenzidine tetrahydrochloride staining (DAB, Cat number G1212, Servicebio, Wuhan, Hubei, China) chromogenic solution was then added; once positive signals were observed under a microscope, the reaction was terminated with distilled water. The cell nuclei were counterstained with hematoxylin for 3–5 minutes. After mounting, images were captured under a microscope.

## 2.7 ELISA Detection

Blood was obtained from anesthetized mice, and the whole blood samples were centrifuged at 3000 rpm at 4 °C for 15 minutes to isolated serum. Serum samples were then used to determine the concentrations of anti-Müllerian hormone (AMH; JONLNBIO, Cat. No. JL16387, Shanghai, China), estradiol (E2; Solarbio Life Sciences, Cat. No. SEKM-0286, Beijing, China), and follicle-stimulating hormone (FSH; JONLNBIO, Cat. No. JL10239, Shanghai, China) using enzyme-linked immunosorbent assay (ELISA) kits, in strict accordance with the manufacturers' instructions.

## 2.8 Western Blot

Total proteins were extracted from ovarian tissue samples using RIPA lysis buffer (Beyotime, Cat. No. P0013B, Shanghai, China), and protein concentrations were determined *via* a bicinchoninic acid (BCA) assay (Beyotime, Cat. No. P0009, Shanghai, China). Equal amounts of protein were separated by sodium dodecyl sulfate-polyacrylamide gel electrophoresis (SDS-PAGE) and then transferred onto polyvinylidene difluoride (PVDF) membranes. The membranes were blocked with 5% non-fat milk in Tris-buffered saline with Tween® 20 (TBST) for 2 hours at room temperature. This was followed by overnight incubation at 4 °C with primary antibodies against the following targets: glyceraldehyde-3-phosphate dehydrogenase (GAPDH; 1:10,000, ABclonal, Cat. No. AC002, Wuhan, China), phosphorylated nuclear factor kappa B (*p*-NF $\kappa$ B; 1:1000, Proteintech, Cat. No. 10745-1-AP, Wuhan, China),

NOD-like receptor pyrin domain-containing 3 (NLRP3; 1:1000, ABclonal, Cat. No. A5652, Wuhan, China), interleukin-1 $\beta$  (IL1 $\beta$ ; 1:1000, ABclonal, Cat. No. A16288, Wuhan, China), and Caspase1 (1:1000, Proteintech, Cat No. 22915-1-AP, Wuhan, China). After three washing with TBST, the membranes were incubated with horseradish peroxidase (HRP)-conjugated secondary antibodies for 2 hours at room temperature. Protein bands were visualized using an enhanced chemiluminescence (ECL) detection system. Densitometric analysis was subsequently performed to quantify the relative expression levels of the target proteins.

## 2.9 The Analysis of qRT-PCR

Total RNA was extracted from ovarian tissue samples using TRIzol® reagent (Beyotime, Cat No. R0016), and RNA concentration and purity were evaluated using a NanoDrop™ spectrophotometer (Thermo Fisher Scientific, Waltham, MA, USA). Complementary DNA (cDNA) was synthesized from 1  $\mu$ g of total RNA using a HiScript II 1st Strand cDNA Synthesis Kit (+gDNA wiper) (Vazyme, Cat No. R212-01, Nanjing, Jiangsu, China), in strict accordance with the manufacturer's instructions. The relative mRNA expression levels of target genes were detected *via* quantitative reverse transcription-polymerase chain reaction (qRT-PCR) using SYBR® Green PCR Master Mix (Vazyme, Cat. No. Q511-02, Nanjing, Jiangsu, China).

The primer sequences are as following:

IL1 $\beta$ : Interleukin 1 beta (NM\_008361.4)

Forward primer: TGCCACCTTTTGACAGTGATG

Reverse primer: AAGGTCCACGGGAAAGACAC

IL18: Interleukin 18 (NM\_008360.2)

Forward primer: TACAAGCATCCAGGCACAGC

Reverse primer: CTGATGCTGGAGGTTGCAGA

NLRP3: NLR family, pyrin domain containing 3 (NM\_145827.4)

Forward primer: GTCACCATGGGTTCTGGTCA

Reverse primer: GGGCTTAGGTCCACACAGAA

Caspase1: caspase 1 (NM\_009807.2)

Forward primer: AACGCCATGGCTGACAAGA

Reverse primer: TGATCACATAGGTCCCGTGC

Actin: Actin beta (NM\_007393.5)

Forward primer: TATAAAACCCGGCGGCGCA

Reverse primer: TCATCCATGGCGAACTGGTG

## 2.10 Statistical Analysis

Data were analyzed using GraphPad Prism software (GraphPad Software Inc., San Diego, CA, USA) and presented as mean  $\pm$  standard error of the mean (SEM). All data were subjected to two-way analysis of variance (ANOVA) followed by Tukey's multiple comparison test, with a *p*-value < 0.05 considered statistically significant. All experiments were performed with at least four biological replicates to ensure the reproducibility of results.

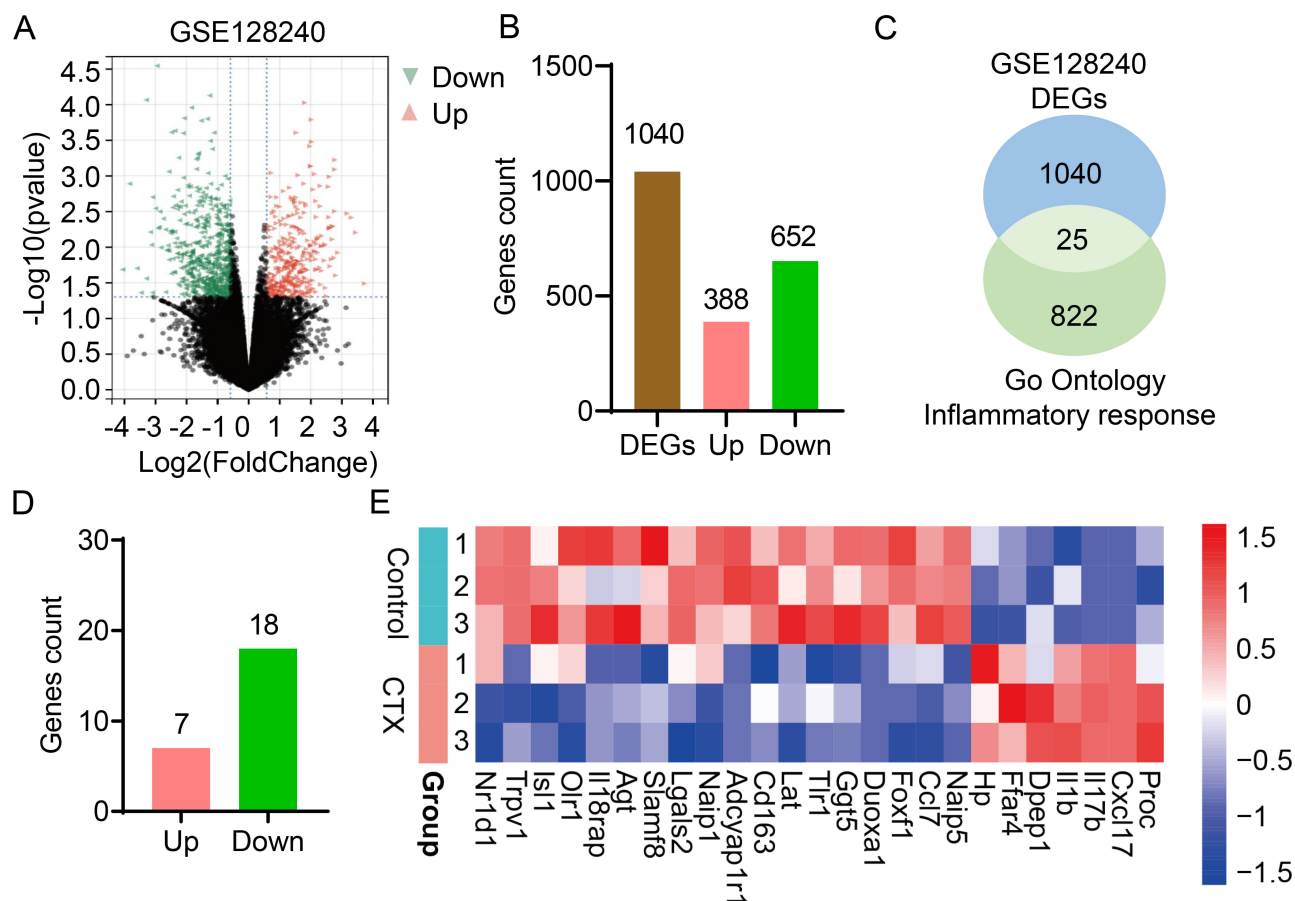


**Fig. 1. Inflammatory candidate genes in premature ovarian insufficiency induced by cyclophosphamide.** (A) Volcano plot of RNA sequencing data from the GSE128240 dataset, showing differentially expressed genes (DEGs) in CTX-induced POI mouse models. (B) The number of upregulated (Pink) and downregulated (Green) DEGs. (C) A Venn diagram illustrates overlap between DEGs from GSE128240 dataset and genes from the “Inflammatory Response” term in the Gene Ontology (GO) database. (D) Detailed gene count of the 25 candidate genes, upregulated (Pink) and downregulated (Green). (E) A heatmap illustrates the expression patterns of the 25 candidate genes across the various samples in the study. CTX, Cyclophosphamide, it is a synthetic alkylating agent chemotherapeutic drug and also a commonly used immunosuppressant in clinical practice.

### 3. Results

#### 3.1 Potential Inflammatory Genes in Cyclophosphamide-Induced Premature Ovarian Insufficiency

To characterize changes in ovarian tissue gene expression following CTX treatment, the RNA sequencing dataset (GSE128240) from CTX-induced POI mouse models was analyzed. Differential gene expression analysis identified 1040 differentially expressed genes (DEGs) in CTX-induced POI, comprising 388 upregulated genes and 652 downregulated genes (Fig. 1A,B). CTX treatment disrupts the balance of ovarian inflammation, which contributes to the onset and progression of POI. To further identify aberrantly expressed inflammatory genes in ovarian tissue, inflammation-related genes were retrieved from the GO database. Subsequent intersection analysis between these inflammation response genes and the DEGs from GSE128240 yielded 25 key inflammatory genes (Fig. 1C).

Of these 25 genes, 7 were upregulated and 18 were downregulated (Fig. 1D), and a heatmap was generated to visualize the expression profiles of these key DEGs (Fig. 1E). In conclusion, integrated analysis of GEO dataset (GSE128240) and GO-derived inflammatory genes enabled the identification of 25 inflammation-associated candidate genes in POI.

#### 3.2 Core Inflammatory Cytokine *IL1β*

To elucidate the regulatory pathways associated with the 25 candidate genes, GO and KEGG enrichment analyses were performed (Fig. 2A,B). The results showed that these candidate genes are significantly enriched in inflammation-related biological processes and signaling pathways, including “Inflammatory Response”, “Neutrophil Chemotaxis”, “Cytokine Activity”, “Cytokine-Cytokine Receptor Interaction”, and the “IL-17 Signaling Pathway” (Fig. 2A,B). To further identify core inflammatory genes



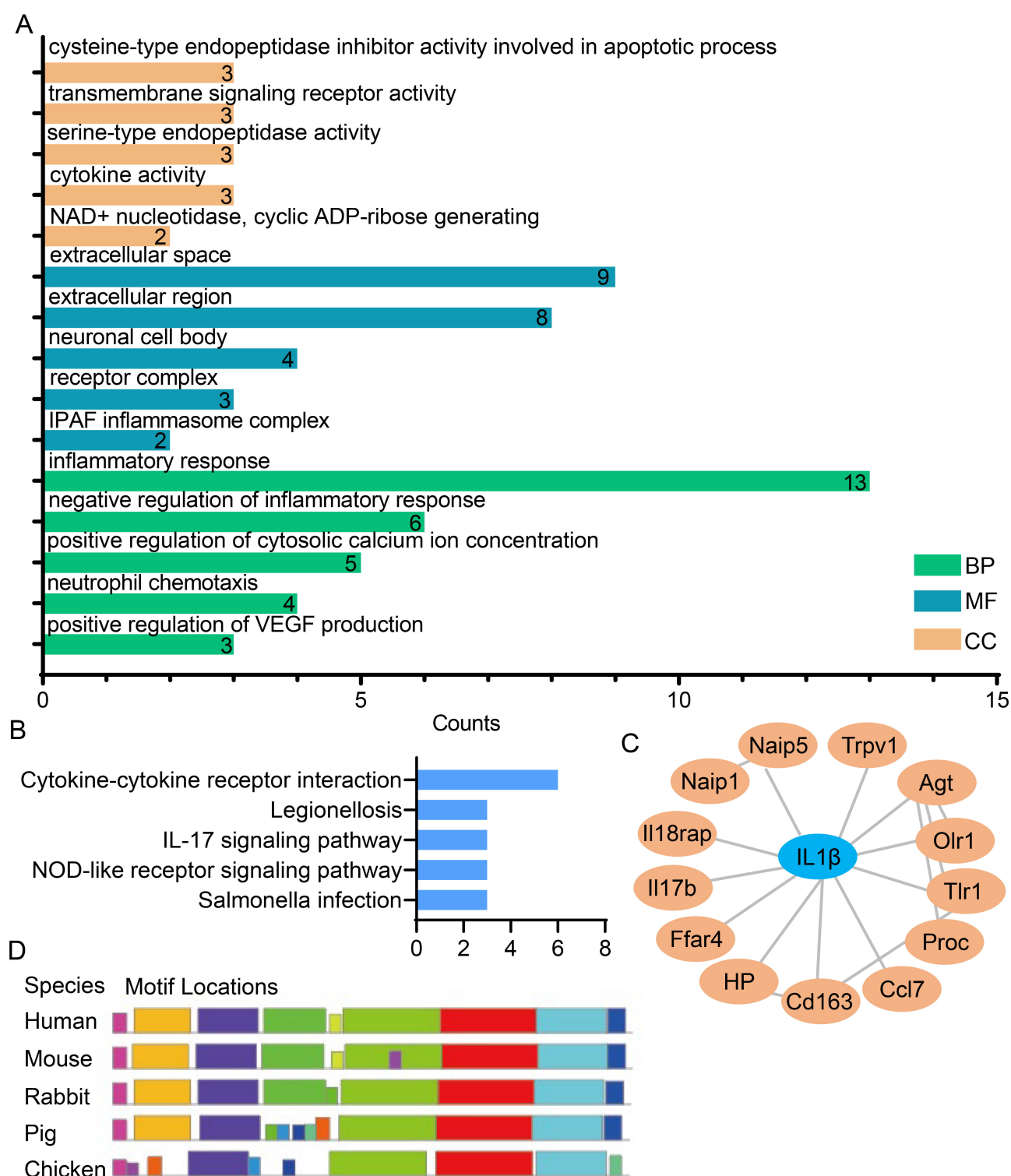


**Fig. 2. Identification and analysis of the core inflammatory IL1 $\beta$ .** (A) GO analysis of the 25 candidate genes, illustrating their enrichment in biological processes (BP), cellular components (CC), and molecular functions (MF). (B) KEGG analysis of the 25 candidate genes, highlighting their involvement in key signaling and metabolic pathways. (C) PPI network construction for the 25 candidate genes, identifying hub proteins and potential interaction modules. (D) Conservation analysis of IL1 $\beta$  motifs across different species. IL1 $\beta$ , interleukin 1 $\beta$ ; KEGG, Kyoto Encyclopedia of Genes and Genomes; PPI, protein-protein interaction.

with this set, PPI network analysis was conducted for the 25 candidate genes using Cytoscape software (Fig. 2C).

This analysis identified IL1 $\beta$  as a hub protein, emphasizing its central role in mediating the inflammatory network

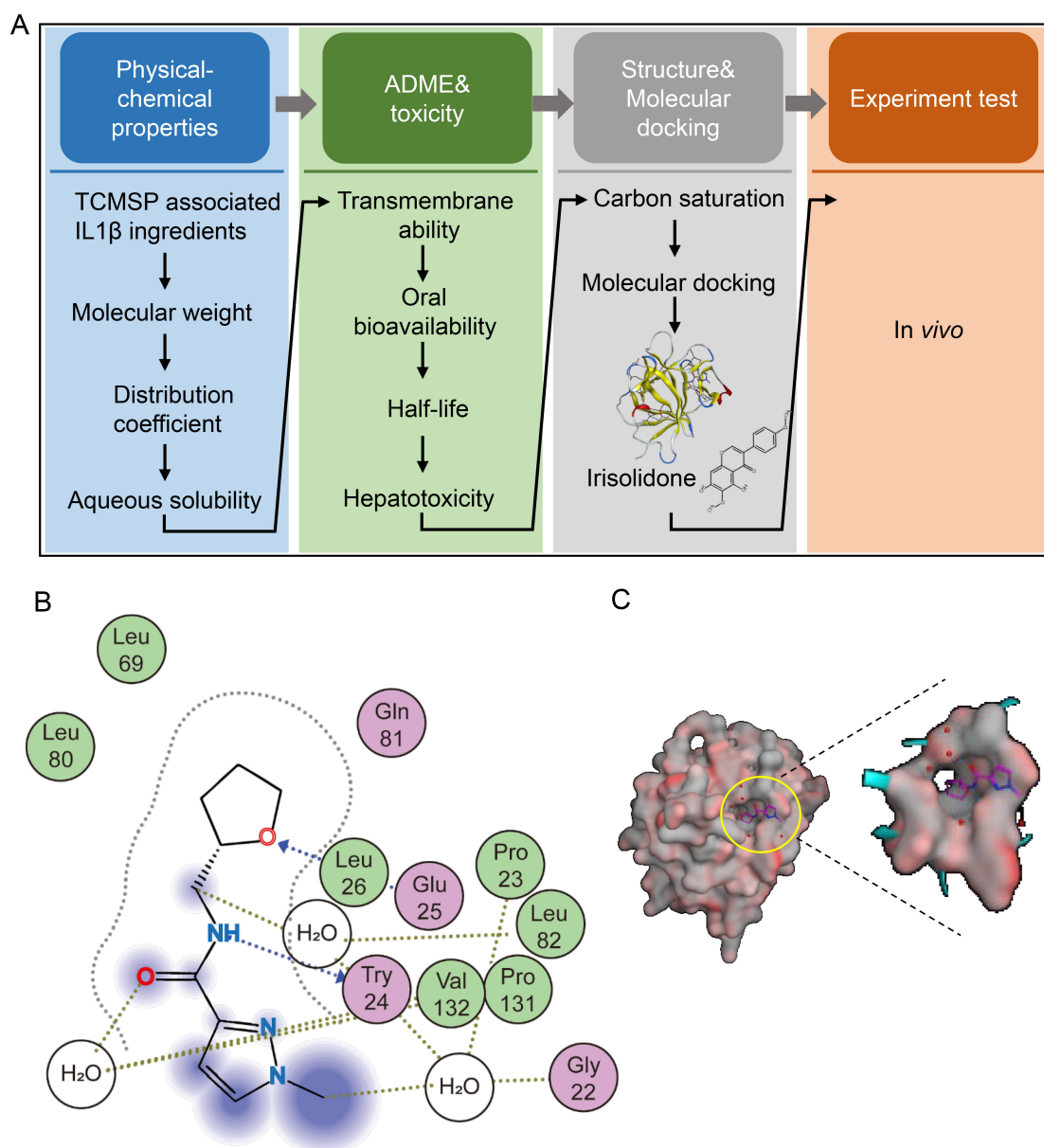


**Fig. 3. Identification of Irisolidone as a natural compound inhibitor of IL1 $\beta$ .** (A) Schematic diagram of the screening process for natural compound inhibitors of IL1 $\beta$ . (B) Two-dimensional (2D) molecular docking diagram showing the binding interactions between Irisolidone and IL1 $\beta$ . The nitrogen atoms at positions 9 and 11 of Irisolidone form hydrogen bonds with the Tyr24 residue of IL1 $\beta$ , with a binding energy of -3.3 kcal/mol. Additionally, the oxygen atom at position 15 of Irisolidone interacts with the Glu25 and Leu26 residues of IL1 $\beta$ , with binding energies of -0.9 kcal/mol and -2.5 kcal/mol, respectively. (C) Three-dimensional (3D) molecular docking model illustrating the binding of Irisolidone within the IL1 $\beta$  binding pocket (The yellow circle shows the magnified view of the binding pocket). Fig. 3B,C were generated using MOE docking software.

(Fig. 2C). Furthermore, motif analysis of IL1 $\beta$  revealed a high level of conservation across species, which underscores its evolutionary significance (Fig. 2D). In summary, through comprehensive functional enrichment and PPI network analyses, we identified IL1 $\beta$  as a core inflammatory cytokine among the 25 candidate genes. These results reveal that IL1 $\beta$  may play a critical role in CTX-induced ovarian inflammation and could be implicated in the pathogenesis of POI.

### 3.3 Irisolidone, an Inhibitor of IL1 $\beta$

To identify natural compound inhibitors of IL1 $\beta$ , a comprehensive search was conducted in the Traditional Chinese Medicine Systems Pharmacology (TCMSP) database, yielding 23 candidate compounds (Fig. 3A). Subsequently, these 23 compounds underwent drug-likeness assessment, which included evaluation of parameters such as “Molecular Weight”, “Distribution Coefficient”, “ADME” (Absorption, Distribution, Metabolism,

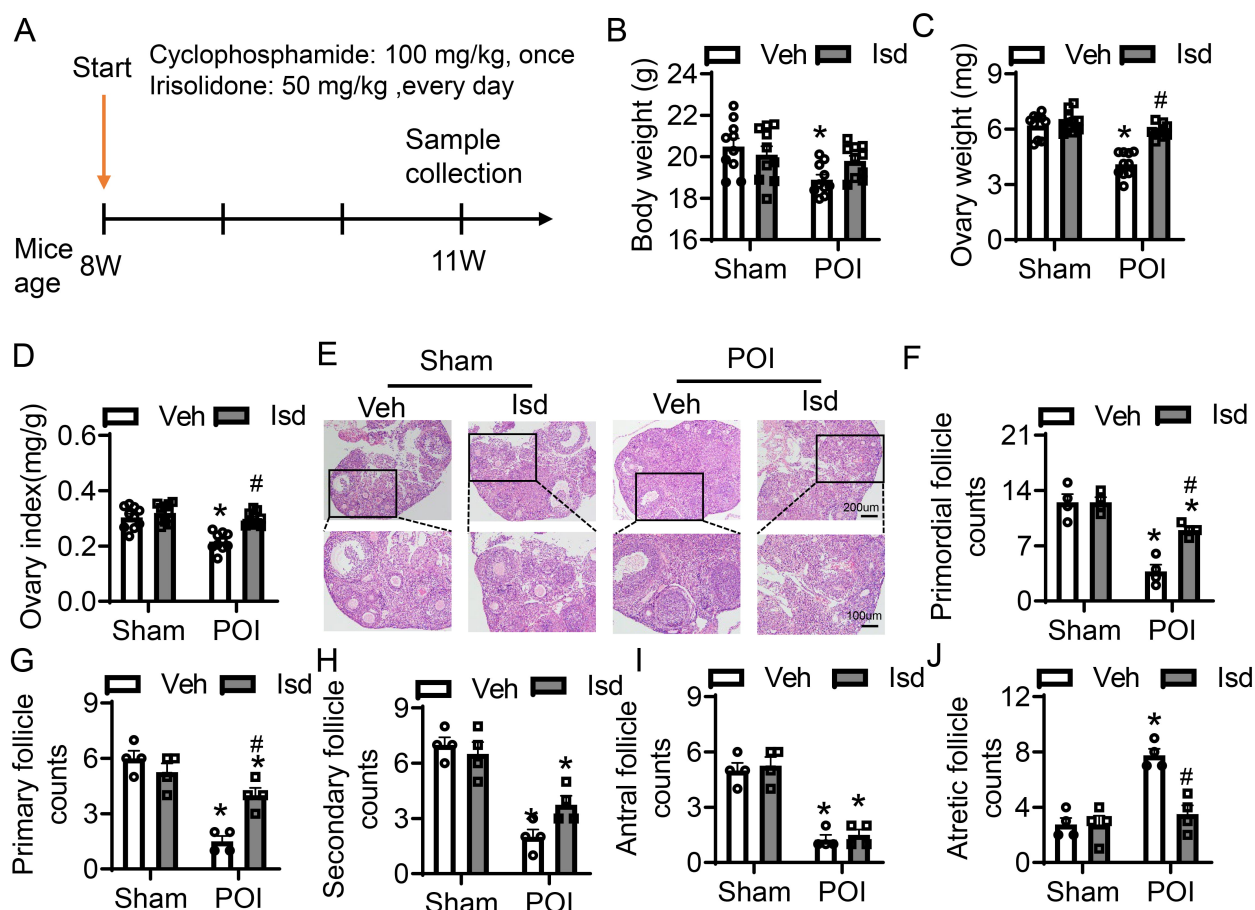


**Fig. 4. Irisolidone ameliorates ovarian folliculogenesis and development with CTX-induced POI.** (A) Schematic diagram of experimental design. (B–D) The body weight (B), ovarian weight (C), and ovarian index (ratio of ovarian weight to body weight) (D) in different groups of mice ( $n = 10$ ). (E) H&E-stained sections of ovarian tissues ( $n = 4$ , The black box is the partial magnified view). Overview figure, scale bar = 200  $\mu\text{m}$ ; Magnified view, scale bar = 100  $\mu\text{m}$ . (F–J) The number of primordial follicles (F), primary follicles (G), secondary follicles (H), antral follicles (I), and atretic follicles (J) in ovarian sections from different groups of mice ( $n = 4$ ). Data are presented as mean  $\pm$  SEM. Statistical analysis was using two-way ANOVA with Tukey's multiple comparison tests. \* $p < 0.05$  vs. Sham-Vehicle group; # $p < 0.05$  vs. POI-Vehicle group. CTX, cyclophosphamide; POI, premature ovarian insufficiency; Veh, vehicle; Isd, Irisolidone; ANOVA, analysis of variance; SEM, standard error of the mean; H&E, Hematoxylin and Eosin.

and Excretion), “Toxicity”, and molecular docking performance. This rigorous screening process ultimately identified Irisolidone as a promising IL1 $\beta$  inhibitor (Fig. 3A). Two-dimensional (2D) molecular docking results revealed that Irisolidone forms hydrogen bonds with specific amino acid residues of IL1 $\beta$ . Specifically, nitrogen atoms at positions 9 and 11 of Irisolidone spontaneously interact with the Tyr24 residue of IL1 $\beta$ , with a binding energy of  $-3.3$  kcal/mol (Fig. 3B). Additionally, oxygen atom at position 15 of Irisolidone interacts with the Glu25 and Leu26 residues of IL1 $\beta$ , with respective binding energies of  $-0.9$  kcal/mol and  $-2.5$  kcal/mol (Fig. 3B). Three-dimensional (3D) molecular docking further demonstrated that Irisolidone can penetrate deep into the IL1 $\beta$  binding pocket, where it interacts effectively with key residues to inhibit IL1 $\beta$  activity (Fig. 3C). In conclusion, systematic screening and molecular docking analyses identified Irisolidone as

a natural IL1 $\beta$  inhibitor. These findings reveal that Irisolidone may inhibit IL1 $\beta$  through stable interactions with critical amino acid residues within its binding pocket. Further *in vivo* studies using mouse models are planned to explore the function of Irisolidone in inflammatory diseases.

### 3.4 Irisolidone Ameliorates CTX-Induced POI

To establish a POI model, 8-week-old female mice were intraperitoneally injected with CTX at 100 mg/kg (Fig. 4A). Mice in the treatment group obtained daily oral administration of Irisolidone (50 mg/kg) for three weeks, after which samples were collected for subsequent analyses (Fig. 4A). Control mice received vehicle treatment only (Fig. 4A). Compared to untreated controls, the control group receiving Irisolidone showed no significant changes in body weight or ovarian weight (Fig. 4B–D). In contrast, the POI group exhibited an obviously reduction in both

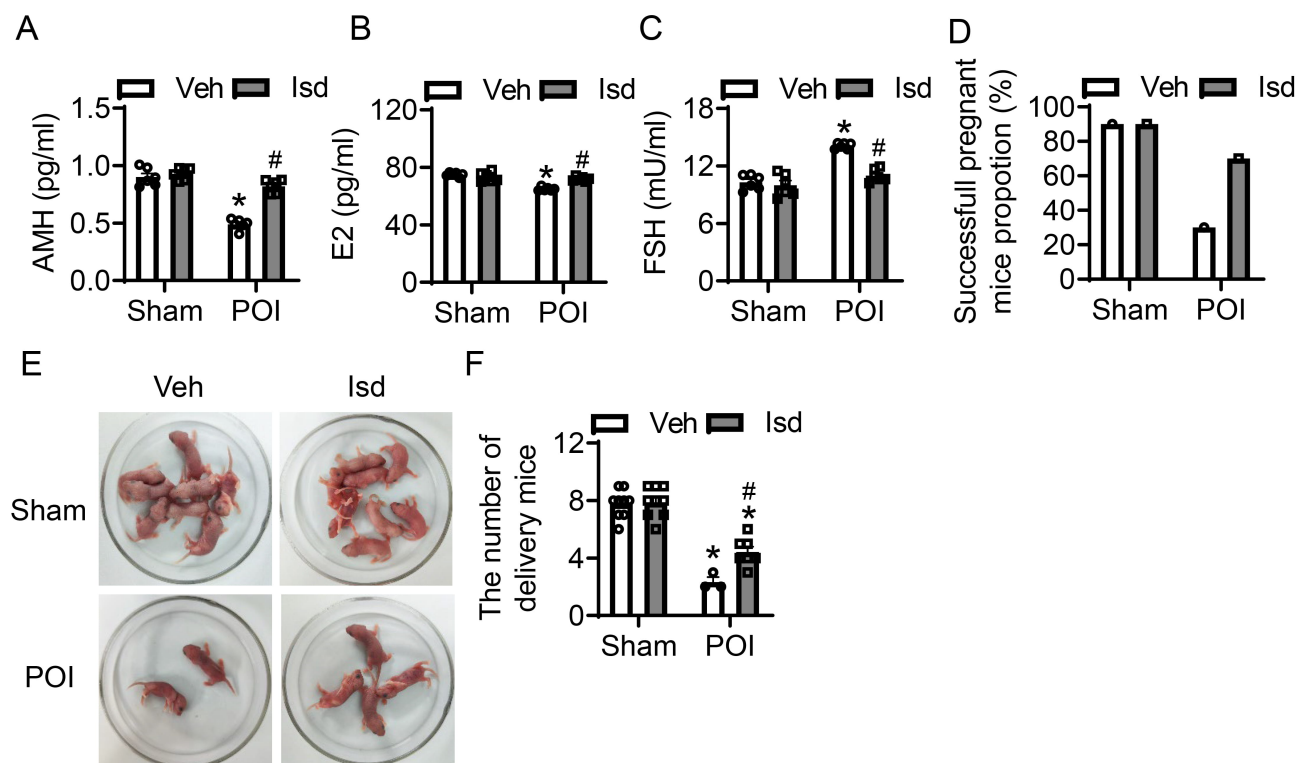


**Fig. 5. Irisolidone restores ovarian function and improves reproductive capacity in mice with CTX-induced POI.** (A–C) The serum levels of anti-Müllerian hormone (AMH) (A), estradiol (E2) (B), and follicle-stimulating hormone (FSH) (C) measured by ELISA in different groups (n = 6). (D–F) The pregnancy rate (D), Diagram representing the number of newborn mice (E), and litter counts (F) in different groups. The number of mice used for each group is as follows: Sham-Vehicle (n = 9), Sham-Irisolidone (n = 9), POI-Vehicle (n = 3), and POI-Irisolidone (n = 7). Data are presented as mean ± SEM. Statistical analysis was using two-way ANOVA with Tukey's multiple comparison tests. \**p* < 0.05 vs. Sham-Vehicle group; #*p* < 0.05 vs. POI-Vehicle group. CTX, cyclophosphamide; POI, premature ovarian insufficiency; Veh, vehicle; Isd, Irisolidone.

body weight and ovarian weight relative to the group. However, Irisolidone treatment significantly improved these parameters, restoring body weight, ovarian weight, and the ovarian index (ratio of ovarian weight to body weight) to near-normal levels (Fig. 4B–D). H&E staining of ovarian tissues revealed abnormal morphology and a reduced number of healthy follicles in the CTX-induced group (Fig. 4E). Irisolidone treatment obviously ameliorated histological damage, preserving ovarian structure and function. We quantified follicles at different developmental stages: primordial, primary, secondary, antral, and atretic follicles. The POI group showed a marked reduction in primordial, primary, secondary, and antral follicles, accompanied by a significantly increased in atretic follicles (Fig. 4F–J). These findings indicate that CTX treatment severely impaired ovarian tissue, leading to abnormal folliculogenesis and reduced fertility. Notably, Irisolidone treatment rescued the number of developing follicles, promoting normal follicular development and reducing the number of atretic follicles (Fig. 4F–J). In summary, experiments *in vivo* demonstrate that Irisolidone treatment significantly mitigates CTX-induced POI-related damage. Irisolidone

improves body weight and ovarian weight, and restores ovarian function by promoting normal follicular development and reducing follicular atresia.

### 3.5 Irisolidone Treatment Restores Ovarian Function and Fertility

Structural abnormalities in ovarian tissue can exert a significantly impact ovarian function and fertility. Follicle-stimulating hormone (FSH), anti-müllerian hormone (AMH), and estradiol (E2) are critical biomarkers for assessing ovarian function, reflecting ovarian reserve, follicular development, and ovulation, respectively. The combination of these three markers enables a comprehensive evaluation of ovarian health. For the purpose of assessing how CTX-induced POI affects ovarian function, we determined the serum levels of FSH, AMH, and E2 in mice through the application of ELISA. Additionally, we evaluated the pregnancy and fertility rates of female mice post-POI induction. In comparison with the control group, administration of CTX led to a significant reduction in serum AMH and E2 levels, whereas serum FSH levels were markedly elevated—findings that are indica-



tive of a substantial decline in ovarian function (Fig. 5A–C). However, Irisolidone treatment significantly reversed these hormonal changes, restoring AMH, E2, and FSH levels to near-normal ranges, thereby improving ovarian function (Fig. 5A–C). To further characterize the effects of POI on reproductive, we assessed pregnancy and fertility in female mice after induction. Relative to controls, CTX treatment resulted in an obvious fall in pregnancy mice, with the count of pups born per pregnant mouse also being markedly decreased (Fig. 5D–F). In contrast, Irisolidone treatment significantly enhanced pregnancy incidence among female mice and elevated the count of pups born per litter (Fig. 5D–F). In summary, our findings demonstrate that Irisolidone possessed therapeutic potential for treating POI, and could provide a promising approach to reinstate ovarian physiological function and improve reproductive capacity in affected individuals.

### 3.6 Irisolidone Modulates the Inflammasome Pathway to Suppress Cyclophosphamide-Induced Abnormal Ovarian Inflammation

Previous pharmacological analysis identified IL1 $\beta$  as a core inflammatory cytokine induced by CTX (Fig. 2C), and Irisolidone was selected as a natural inhibitor of IL1 $\beta$  (Fig. 3). For the purpose of further investigating how Irisolidone exerts its inhibitory effect on IL1 $\beta$ , we assessed the expression levels of two key inflammatory cytokines IL1 $\beta$  and IL18 in ovarian tissues and serum. The results showed that CTX significantly increased the expression of IL1 $\beta$  and IL18 in both ovarian tissues and circulation in the POI group, and Irisolidone treatment markedly reversed this upregulation (Fig. 6A–D). In addition, we conducted a further examination of IL1 $\beta$  expression at the protein level. Our findings revealed a marked upregulation of IL1 $\beta$  in ovarian tissues of CTX-induced POI, which serves to validate the reliability of the GSE128240 dataset (Fig. 6E,F). IL1 $\beta$  and IL18 are regulated by the inflammasome pathway, which involves NF $\kappa$ B, NLRP3, and Caspase1. We first assessed the phosphorylation status of NF $\kappa$ B, a key regulator of inflammation. The findings demonstrated that CTX significantly led to a notable elevation of *p*-NF $\kappa$ B, while Irisolidone treatment effectively inhibited this increase (Fig. 6E,G). It is well established that *p*-NF $\kappa$ B translocates into the nuclear compartment, and once localized there, it promotes the transcriptional activity of NLRP3, pro-IL1 $\beta$ , and pro-IL18 [20]. Increased NLRP3 expression facilitates the assembly of the NLRP3 inflammasome complex within cytoplasm, thereby triggering the conversion of pro-Caspase1 to its mature functional form [21]. This mature Caspase1 mediates the cleavage of pro-IL1 $\beta$  and pro-IL18 into their biologically active isoforms, resulting in elevated levels of IL1 $\beta$  and IL18 [22]. The data show that CTX induced an obviously upregulated NLRP3 and Caspase1 expression. In contrast, administration of Irisolidone exerted a notable inhibitory effect

on the expression of these two proteins (NLRP3 and Caspase1), bringing their levels back to a state close to normal (Fig. 6E,H,I). In addition, it was found that Irisolidone downregulated the mRNA expression of *Nlrp3* and *Caspase1*, which reveals its inhibitory effect on inflammation (Fig. 6J,K). Additionally, IHC staining of *p*-NF $\kappa$ B, NLRP3, and Caspase1 showed that the expression of the inflammatory pathway in the ovarian tissues of mice with POI was significantly increased compared with the control group, while treatment with Irisolidone significantly inhibited the activation of this inflammatory pathway (Fig. 6L). To summarize, the results illustrate that Irisolidone significantly inhibits aberrant regulation of *p*-NF $\kappa$ B/NLRP3/Caspase1 pathway induced by CTX. By suppressing this pathway, Irisolidone reduces the expression of downstream inflammatory cytokines IL1 $\beta$  and IL18, thereby restoring the inflammatory balance in ovarian tissue. This mechanistic insight highlights the therapeutic potential of Irisolidone in mitigating CTX-induced POI and preserving ovarian function.

## 4. Discussion

Our study focused on CTX induced POI, particularly the abnormal inflammation in the ovaries. Through the intersection of RNA sequencing data (GSE128240) derived from the ovarian tissues of CTX-treated mice and inflammation-related genes from the GO database, we identified 25 candidate genes (Fig. 1). Subsequent PPI analysis revealed IL1 $\beta$  as a core inflammatory gene (Fig. 2). Additionally, after further screening of natural compounds for their anti-inflammatory activities, Irisolidone was recognized as a promising potential therapeutic candidate (Fig. 3). The studies *in vivo* demonstrated that Irisolidone treatment improved CTX-induced abnormalities in ovarian cell development, ovarian function, and fertility (Figs. 4,5). Follow-up experiments showed that Irisolidone suppresses the *p*-NF $\kappa$ B/NLRP3/Caspase1 pathway by reducing the expression of inflammatory cytokines IL18 and IL1 $\beta$ , thereby alleviating ovarian tissue inflammation (Figs. 6,7). In summary, our research identifies Irisolidone as a potential therapeutic agent for CTX-induced POI and elucidates its mechanism of action in mitigating ovarian inflammatory dysregulation.

Clinical anticancer therapeutic regimens frequently contribute to the development of POI and subsequent infertility [23]. Commonly used chemotherapeutic agents include cyclophosphamide, cisplatin, and doxorubicin [24, 25]. Our study specifically focused on POI induced by cyclophosphamide, and whether Irisolidone can mitigate POI caused by other chemotherapy drugs remains to be determined. Cyclophosphamide-induced POI is influenced by multiple factors, including DNA damage [26], oxidative stress, cellular senescence [27], apoptosis [28], mitochondrial autophagy [29], and pyroptosis [30]. While our research has concentrated on the abnormal inflammation in

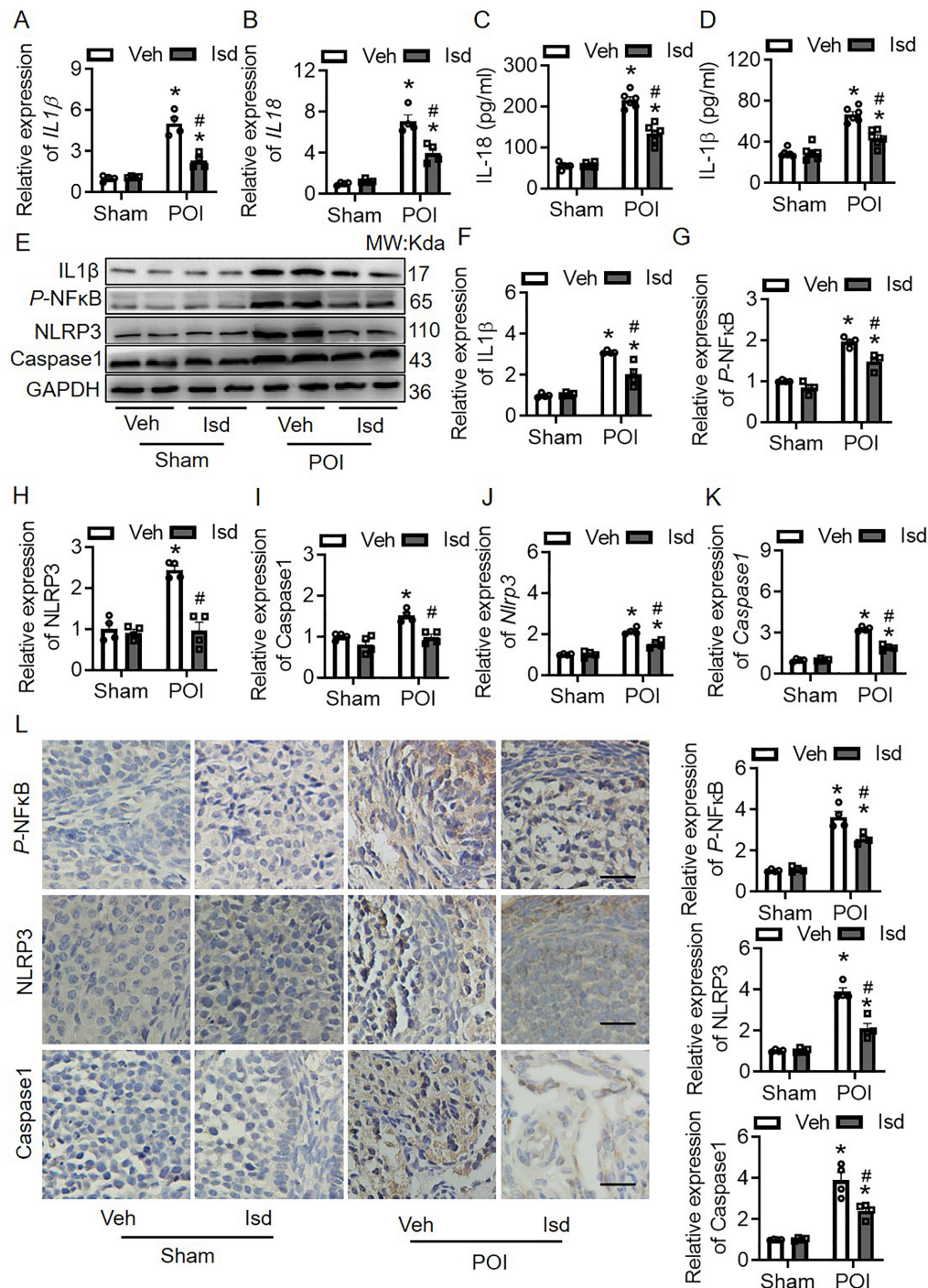


**Fig. 6. Irisolidone inhibits the dysregulation of inflammatory cytokines by regulating NFκB/NLRP3/Caspase1 axis.** (A,B) IL1β (A) and IL18 (B) at mRNA level, as determined by qRT-PCR (n = 4). (C,D) IL1β (C) and IL18 (D) in mouse serum, as measured by ELISA (n = 6). (E–I) Representative images and quantification the protein expression of IL1β, p-NFκB, NLRP3, and Caspase1 (n = 4). (J,K) The mRNA expression of Nlrp3 and Caspase1 in ovarian tissues (n = 4). (L) The IHC staining of p-NFκB, NLRP3, and Caspase1 in ovarian tissue section (n = 4). Scale bar = 20 μm. Data are presented as mean ± SEM. Statistical analysis was using two-way ANOVA with Tukey's multiple comparison tests. \**p* < 0.05 vs. Sham-Vehicle group; #*p* < 0.05 vs. POI-Vehicle group. CTX, cyclophosphamide; POI, premature ovarian insufficiency; Veh, vehicle; Isd, Irisolidone; NF-κB, nuclear factor kappa B; IL18, Interleukin 18; qRT-PCR, quantitative reverse transcription-polymerase chain reaction; NLRP3, NOD-like receptor pyrin domain-containing 3; IHC, Immunohistochemistry.

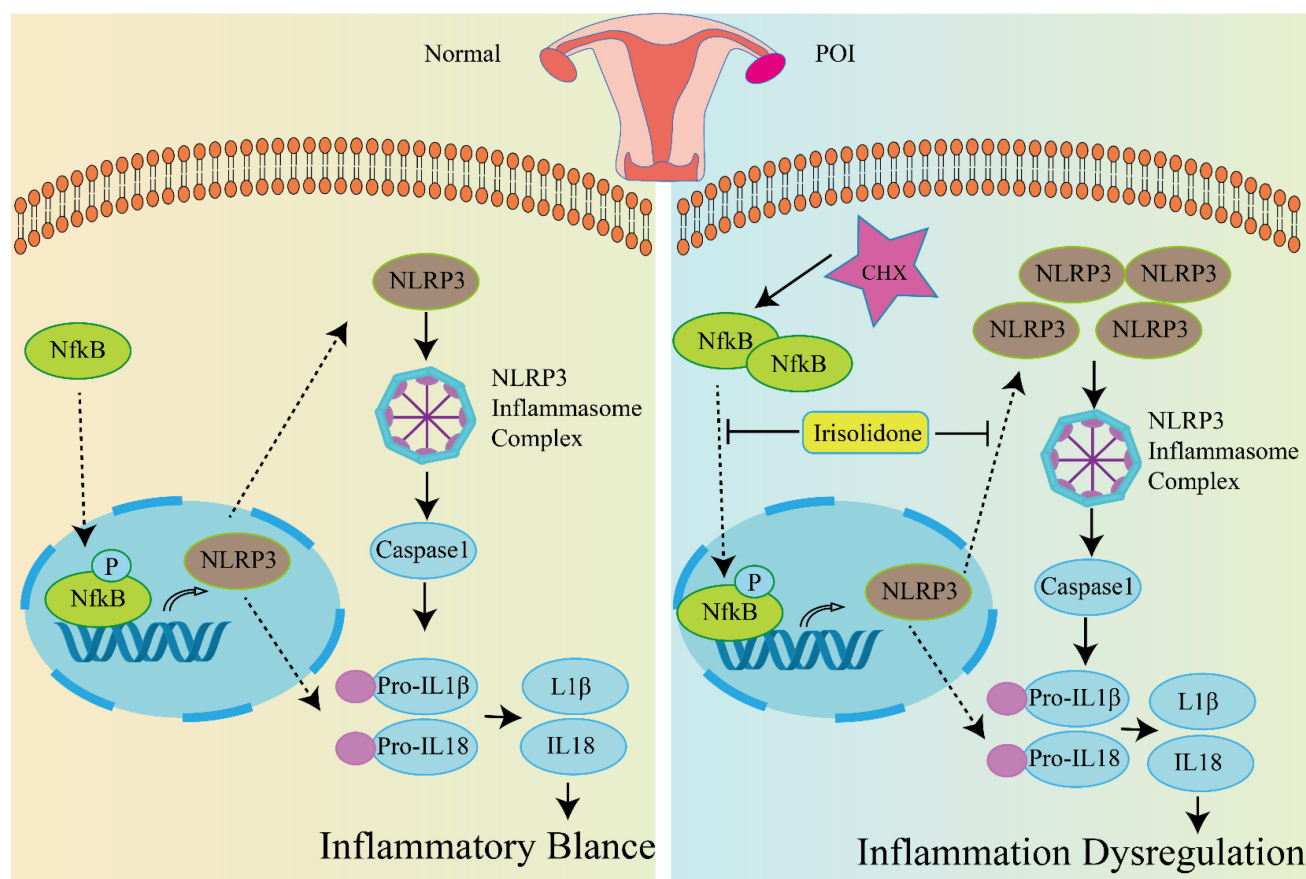


**Fig. 7. The underlying mechanism of Irisolidone protects against POI caused by CTX.** In healthy conditions, the inflammasome pathway maintains a balanced state of inflammation within the body. Upon treatment with CTX, ovarian tissue undergoes premature ovarian insufficiency (POI). CTX triggers the phosphorylation of  $\text{NF}\kappa\text{B}$  as well as its translocation into nucleus, an effect that in turn promotes the enhanced transcription of NLRP3. Subsequently, NLRP3 not only upregulates pro-IL1 $\beta$  and pro-IL18 expression but also facilitates the assembly of NLRP3 Inflammasome, which mediates the conversion of pro-Caspase1 into its mature form. Once activated, Caspase1 proceeds to cleave pro-IL1 $\beta$  and pro-IL18 into mature bioactive isoforms, ultimately resulting in the overproduction of IL1 $\beta$  and IL18. This subsequently gives rise to abnormal inflammatory responses in ovarian tissue, a phenomenon that impairs folliculogenesis and compromises ovarian function. Irisolidone treatment exerts a protective effect by modulating the  $\text{NF}\kappa\text{B}$ /NLRP3/Caspase1 pathway. Irisolidone suppresses the phosphorylation and nuclear entry of  $\text{NF}\kappa\text{B}$ , thereby reducing the transcriptional activity of NLRP3 as well as its cytoplasmic expression, and thus hindering the assembly of the NLRP3 inflammasome. With reducing levels of mature Caspase1, the cleavage of pro-IL1 $\beta$  and pro-IL18 into their active forms is diminished, leading to decreased expression of IL1 $\beta$  and IL18. Ultimately, Irisolidone restores the inflammatory balance in the ovarian tissue, mitigating the adverse effects of CTX-induced POI and preserving normal ovarian function and follicular development. Fig. 7 was created with Adobe Illustrator CC (Adobe Inc., San Jose, CA, USA).

the ovaries caused by CTX, the potential of Irisolidone to address other pathogenic factors induced by CTX, such as those mentioned above, requires further investigation.

Through network pharmacology approaches and molecular docking simulations, we identified Irisolidone as a potential drug candidate. Nevertheless, the binding energy between Irisolidone and the inflammatory cytokine IL1 $\beta$  was merely  $-3.3$  kcal/mol that indicates the interaction strength is insufficient to support optimal therapeutic effectiveness. Therefore, future work will focus on the molecular optimization of Irisolidone to enhance its binding affinity to IL1 $\beta$ .

Our findings indicate that Irisolidone can inhibit the CTX-induced elevation of  $p\text{-NF}\kappa\text{B}$  and Caspase1. The phosphorylation and nuclear translocation of  $\text{NF}\kappa\text{B}$  activate downstream transcription factors, leading to increased autophagy. Abnormal increases in autophagy can negatively impact follicle development [31]. This suggests that Irisolidone may suppress CTX-induced aberrant autophagy, thereby restoring the normal development of follicular cells. Additionally, the upregulation of Caspase1 leads to increased expression of Gasdermin, promoting the occurrence of pyroptosis [32]. This implies that Irisolidone might also have the potential to inhibit pyroptosis by sup-



pressing Caspase1 activity. In summary, our research indicates that Irisolidone could potentially mitigate both abnormal autophagy and pyroptosis induced by CTX. Our future studies will expand on these findings to determine whether Irisolidone has therapeutic effects on autophagy and pyroptosis, as well as to explore its broader implications in treating CTX-induced premature ovarian insufficiency.

## 5. Conclusion

To conclude, our study confirmed that Irisolidone is effective in treating CTX-induced POI. By inhibiting the activation of *p*-NF $\kappa$ B and Caspase1, Irisolidone mitigates abnormal inflammation, autophagy, and pyroptosis, thereby restoring ovarian function and follicular development. These results indicate that Irisolidone shows potential as a new therapeutic agent for POI, providing a promising novel approach for the clinical treatment of this disorder.

## Availability of Data and Materials

The datasets used and analyzed during the current study are available from the corresponding author on reasonable request. The RNA sequencing data of CTX-Induced POI was from GEO data (GSE128240).

## Author Contributions

SYM designed the study. MJL, ZHW, XHC, HFW, XH, YPP performed the experiments and collected data. JYC established the animal model. MJL wrote the paper and SYM revised the manuscript. All authors contributed to editorial changes in the manuscript. All authors read and approved the final manuscript. All authors have participated sufficiently in the work and agreed to be accountable for all aspects of the work.

## Ethics Approval and Consent to Participate

All animal experiments were followed the NIH guide for the care and use of laboratory animals (NIH Publication No. 80-23; revised 1978). All animal experiment were approved by the Animal Experimental Ethical Inspection Form at Guizhou Medical University (No. 12403436). We confirm the authenticity of this statement.

## Acknowledgment

Not applicable.

## Funding

This study was supported by Healthcare Research Project of Gansu Province (GSWSKY2022-17) and Research fund project of Gansu Provincial Hospital (20GSSY4-40).

## Conflict of Interest

The authors declare no conflict of interest.

## References

- [1] McDonald IR, Welt CK, Dwyer AA. Health-related quality of life in women with primary ovarian insufficiency: a scoping review of the literature and implications for targeted interventions. *Human Reproduction* (Oxford, England). 2022; 37: 2817–2830. <https://doi.org/10.1093/humrep/deac200>.
- [2] Golezar S, Ramezani Tehrani F, Khazaei S, Ebadi A, Keshavarz Z. The global prevalence of primary ovarian insufficiency and early menopause: a meta-analysis. *Climacteric: the Journal of the International Menopause Society*. 2019; 22: 403–411. <https://doi.org/10.1080/13697137.2019.1574738>.
- [3] Nguyen HH, Milat F, Vincent AJ. New insights into the diagnosis and management of bone health in premature ovarian insufficiency. *Climacteric: the Journal of the International Menopause Society*. 2021; 24: 481–490. <https://doi.org/10.1080/13697137.2021.1917539>.
- [4] Podfigurna A, Męczekalski B. Cardiovascular health in patients with premature ovarian insufficiency. Management of long-term consequences. *Przegląd Menopauzalny = Menopause Review*. 2018; 17: 109–111. <https://doi.org/10.5114/pm.2018.78551>.
- [5] Wang H, Chen H, Qin Y, Shi Z, Zhao X, Xu J, *et al.* Risks associated with premature ovarian failure in Han Chinese women. *Reproductive Biomedicine Online*. 2015; 30: 401–407. <https://doi.org/10.1016/j.rbmo.2014.12.013>.
- [6] Hickey M, Basu P, Sassarini J, Stegmann ME, Weiderpass E, Nakawala Chilowa K, *et al.* Managing menopause after cancer. *Lancet* (London, England). 2024; 403: 984–996. [https://doi.org/10.1016/S0140-6736\(23\)02802-7](https://doi.org/10.1016/S0140-6736(23)02802-7).
- [7] Su C, Zhang R, Zhang X, Lv M, Liu X, Ao K, *et al.* Dingkun Pill modulate ovarian function in chemotherapy-induced premature ovarian insufficiency mice by regulating PTEN/PI3K/AKT/FOXO3a signaling pathway. *Journal of Ethnopharmacology*. 2023; 315: 116703. <https://doi.org/10.1016/j.jep.2023.116703>.
- [8] van Dorp W, Haupt R, Anderson RA, Mulder RL, van den Heuvel-Eibrink MM, van Dulmen-den Broeder E, *et al.* Reproductive Function and Outcomes in Female Survivors of Childhood, Adolescent, and Young Adult Cancer: A Review. *Journal of Clinical Oncology: Official Journal of the American Society of Clinical Oncology*. 2018; 36: 2169–2180. <https://doi.org/10.1200/JCO.2017.76.3441>.
- [9] Cartwright B, Grace J, Rymer J. A clinical dilemma: the potential use of egg freezing to preserve fertility in a young patient at risk of developing premature ovarian failure. *Menopause International*. 2010; 16: 65–67. <https://doi.org/10.1258/mi.2010.010015>.
- [10] Ebrahimi M, Akbari Asbagh F. The role of autoimmunity in premature ovarian failure. *Iranian Journal of Reproductive Medicine*. 2015; 13: 461–472.
- [11] Boots CE, Jungheim ES. Inflammation and Human Ovarian Follicular Dynamics. *Seminars in Reproductive Medicine*. 2015; 33: 270–275. <https://doi.org/10.1055/s-0035-1554928>.
- [12] Keskin-Aktan A, Kutlay Ö. Exogenous Apelin-13 Administration Ameliorates Cyclophosphamide- Induced Oxidative Stress, Inflammation, and Apoptosis in Rat Lungs. *Protein and Peptide Letters*. 2023; 30: 743–753. <https://doi.org/10.2174/0929866530666230824142516>.
- [13] Iqbal A, Najmi AK, Md S, Alkreathy HM, Ali J, Syed MA, *et al.* Oral delivery of nerolidol alleviates cyclophosphamide-induced renal inflammation, apoptosis, and fibrosis via modulation of NF- $\kappa$ B/cleaved caspase-3/TGF- $\beta$  signaling molecules. *Drug Delivery*. 2023; 30: 2241661. <https://doi.org/10.1080/10717544.2023.2241661>.
- [14] Iqbal A, Sharma S, Ansari MA, Najmi AK, Syed MA, Ali J, *et al.* Nerolidol attenuates cyclophosphamide-induced cardiac in-



- inflammation, apoptosis and fibrosis in Swiss Albino mice. *European Journal of Pharmacology*. 2019; 863: 172666. <https://doi.org/10.1016/j.ejphar.2019.172666>.
- [15] Yao Y, Wang B, Yu K, Song J, Wang L, Yang X, *et al*. Nur77 ameliorates cyclophosphamide-induced ovarian insufficiency in mice by inhibiting oxidative damage and cell senescence. *Journal of Ovarian Research*. 2024; 17: 203. <https://doi.org/10.1186/s13048-024-01532-y>.
- [16] Li Q, An X, Man X, Chu M, Zhao T, Yu H, *et al*. Transcriptome analysis reveals that cyclophosphamide induces premature ovarian failure by blocking cholesterol biosynthesis pathway. *Life Sciences*. 2019; 239: 116999. <https://doi.org/10.1016/j.lfs.2019.116999>.
- [17] Liu H, Wang J, Zhou W, Wang Y, Yang L. Systems approaches and polypharmacology for drug discovery from herbal medicines: an example using licorice. *Journal of Ethnopharmacology*. 2013; 146: 773–793. <https://doi.org/10.1016/j.jep.2013.02.004>.
- [18] Ru J, Li P, Wang J, Zhou W, Li B, Huang C, *et al*. TCMSP: a database of systems pharmacology for drug discovery from herbal medicines. *Journal of Cheminformatics*. 2014; 6: 13. <https://doi.org/10.1186/1758-2946-6-13>.
- [19] Rodgers RJ, Irving-Rodgers HF. Morphological classification of bovine ovarian follicles. *Reproduction* (Cambridge, England). 2010; 139: 309–318. <https://doi.org/10.1530/REP-09-0177>.
- [20] Broz P, Dixit VM. Inflammasomes: mechanism of assembly, regulation and signalling. *Nature Reviews. Immunology*. 2016; 16: 407–420. <https://doi.org/10.1038/nri.2016.58>.
- [21] Jo EK, Kim JK, Shin DM, Sasakawa C. Molecular mechanisms regulating NLRP3 inflammasome activation. *Cellular & Molecular Immunology*. 2016; 13: 148–159. <https://doi.org/10.1038/cmi.2015.95>.
- [22] Shao BZ, Xu ZQ, Han BZ, Su DF, Liu C. NLRP3 inflammasome and its inhibitors: a review. *Frontiers in Pharmacology*. 2015; 6: 262. <https://doi.org/10.3389/fphar.2015.00262>.
- [23] Anderson RA, Brewster DH, Wood R, Nowell S, Fischbacher C, Kelsey TW, *et al*. The impact of cancer on subsequent chance of pregnancy: a population-based analysis. *Human Reproduction* (Oxford, England). 2018; 33: 1281–1290. <https://doi.org/10.1093/humrep/dey216>.
- [24] Spears N, Lopes F, Stefansdottir A, Rossi V, De Felici M, Anderson RA, *et al*. Ovarian damage from chemotherapy and current approaches to its protection. *Human Reproduction Update*. 2019; 25: 673–693. <https://doi.org/10.1093/humupd/dmz027>.
- [25] Lobo RA. Hormone-replacement therapy: current thinking. *Nature Reviews. Endocrinology*. 2017; 13: 220–231. <https://doi.org/10.1038/nrendo.2016.164>.
- [26] Luan Y, Yu SY, Abazarikia A, Dong R, Kim SY. TAp63 determines the fate of oocytes against DNA damage. *Science Advances*. 2022; 8: eade1846. <https://doi.org/10.1126/sciadv.ade1846>.
- [27] Ai G, Meng M, Guo J, Li C, Zhu J, Liu L, *et al*. Adipose-derived stem cells promote the repair of chemotherapy-induced premature ovarian failure by inhibiting granulosa cells apoptosis and senescence. *Stem Cell Research & Therapy*. 2023; 14: 75. <https://doi.org/10.1186/s13287-023-03297-5>.
- [28] Li T, Liu J, Liu K, Wang Q, Cao J, Xiao P, *et al*. Alpha-ketoglutarate ameliorates induced premature ovarian insufficiency in rats by inhibiting apoptosis and upregulating glycolysis. *Reproductive Biomedicine Online*. 2023; 46: 673–685. <https://doi.org/10.1016/j.rbmo.2023.01.005>.
- [29] Hu B, Zheng X, Zhang W. Resveratrol- $\beta$ cd inhibited premature ovarian insufficiency progression by regulating granulosa cell autophagy. *Journal of Ovarian Research*. 2024; 17: 18. <https://doi.org/10.1186/s13048-024-01344-0>.
- [30] Chen Y, Zhao Y, Miao C, Yang L, Wang R, Chen B, *et al*. Quercetin alleviates cyclophosphamide-induced premature ovarian insufficiency in mice by reducing mitochondrial oxidative stress and pyroptosis in granulosa cells. *Journal of Ovarian Research*. 2022; 15: 138. <https://doi.org/10.1186/s13048-022-01080-3>.
- [31] Kumariya S, Ubba V, Jha RK, Gayen JR. Autophagy in ovary and polycystic ovary syndrome: role, dispute and future perspective. *Autophagy*. 2021; 17: 2706–2733. <https://doi.org/10.1080/15548627.2021.1938914>.
- [32] Shi J, Gao W, Shao F. Pyroptosis: Gasdermin-Mediated Programmed Necrotic Cell Death. *Trends in Biochemical Sciences*. 2017; 42: 245–254. <https://doi.org/10.1016/j.tibs.2016.10.004>.